Int J Clin Exp Pathol 2016;9(4):4891-4900
www.ijcep.com /ISSN:1936-2625/IJCEP0024078

Original Article

Advanced glycation end products induced the epithelial-mesenchymal transition in retinal pigment epithelial cells via ERK activation

Xiao-Li Chen*, Yu-Jing Bai*, Qin-Rui Hu, Lv-Zhen Huang, Xiao-Xin Li

*Department of Ophthalmology, Peking University People's Hospital, Key Laboratory of Vision Loss and Restoration, Ministry of Education, Beijing Key Laboratory for The Diagnosis and Treatment of Retinal and Choroid Diseases, Beijing, China. *Equal contributors and co-first authors.*

Received January 15, 2016; Accepted March 26, 2016; Epub April 1, 2016; Published April 15, 2016

Abstract: Proliferative diabetic retinopathy (PDR), an end-stage diabetic complication, accounts for blindness and low vision in most diabetic patients. Advanced glycation end products (AGEs) and the epithelial-mesenchymal transition (EMT) of retinal pigment epithelial (RPE) cells are associated with the development of PDR via multifactorial mechanisms. However, whether AGEs can induce the EMT in RPE cells was previously unknown. In this study, we found that AGEs induced the EMT, accompanied by a decreased expression of the epithelial marker ZO-1, increased the expression of the mesenchymal marker fibronectin, elevated the production of EMT-related cytokines such as vascular endothelial growth factor (VEGF) and interleukin-6, and enhanced cell migration ability. Furthermore, the AGEs-induced EMT could be partly reversed by using an inhibitor of ERK activation, U0126. We also found that AGEs could regulate cell apoptosis and the cell cycle while promoting cell phenotype transformation from a typical cobblestone-like to a fibroblast-like morphology. Collectively, these data suggest that AGEs participate in the pathogenesis of PDR by inducing the EMT in an ERK-dependent pathway. Additional studies investigating the role of AGEs in the EMT may be promising for the prevention and treatment of PDR.

Keywords: Advanced glycation end products, epithelial-mesenchymal transition, proliferative diabetic retinopathy, ERK, RPE cells

Introduction

Diabetic retinopathy (DR) is a major cause of blindness and low vision in the elderly worldwide. Proliferative diabetic retinopathy (PDR), the advanced stage of DR and the most serious ocular complication of diabetes, can cause hemorrhages, retinal detachment and total blindness [1]. PDR is a wound healing-like response in which fibrotic epiretinal membranes are formed either on the surface of the retina or within the vitreous, accompanied by an influx of inflammatory cytokines and angiogenic factors into the retina [2]. The epiretinal membranes consist of various cell types, including retinal pigment epithelial (RPE) cells, which have a fibroblast-like morphology, undergo the epithelial-mesenchymal transition (EMT) and are considered to be contractile, leading to the contraction of epiretinal membranes and subsequently toretinal detachment [3, 4].

EMT is a process in which epithelial cells undergo a transition from their differentiated morphology to a mesenchymal-like phenotype and occurs during embryonic development, tumor metastasis, wound healing, and organ fibrosis [5]. This transition is characterized by a loss of cell-cell contacts, down-regulation of epithelial cell markers such as ZO-1, and up-regulation of mesenchymal markers such as fibronectin [6]. Additionally, EMT is associated with enhanced cell migration and the subsequent aggravation ofthe pathologic fibrosis process in the proliferative diseases of the eye, heart, kidney, liver, and lung [7]. In recent studies, increasing evidence has shown that the EMT of RPE cells contributes to the development of PDR [8, 9]; however, the mechanism underlying the EMT is largely unknown.

Advanced glycation end products (AGEs) may participate in the pathogenesis of numerous

diseases, including diabetic complications, aging and atherosclerosis [10]. Recently, a considerable number of studies have suggested that AGEs might play a pivotal role in diabetic retinopathy. Elevated levels of AGEs in the vitreous of patients with PDR were reported [11]. *In vitro* studies showed that AGEs induced the production of vascular endothelial growth factor (VEGF) in cultured retinal Müller cells and RPE cells [12, 13]. An *in vivo* study showed that the injection of glycated albumin (Alb-AGE) into mice increases VEGF mRNA expression in the eyes, contributing to the development of DR [14]. Our study also found that the expression of the AGE receptor (RAGE) is increased in the retinas of type 2 diabetic rats and in high-glucose-treated ARPE-19 cells [15]. Although the EMT is crucial to the development and progression of PDR, few reports have describedthe effect of AGEs on the EMT in RPE cells. Therefore, the present study aimed to investigate whether AGEs could induce the EMT in human RPE cells and the underlying molecular mechanisms.

Materials and methods

Reagents and cell culture

AGEs were purchased from RD (Minneapolis, MN, US), and U0126 was purchased from Sigma (St. Louis, MO, US). A cell apoptosis and cell cycle kit was obtained from BD Biosciences (Bedford, MA, US). Anti-β-actin, anti-extracellular signal-related kinase (ERK), anti-phospho ERK, anti-zonula occludens-1 (ZO-1), and anti-fibronectin were obtained from Cell Signaling Technology (Danvers, MA, US). Goat anti-rabbit fluorescein isothiocyanate (FITC)-conjugated secondary antibodies were purchased from Molecular Probes (Invitrogen, Carlsbad, CA, US). A Cell Counting Kit-8 (CCK-8) and Transwell product were purchased from Dojindo (Shanghai, China) and Corning (Tewksbury, MA, US), respectively.

The human RPE cell line ARPE-19 was obtained from the American Type Culture Collection (ATCC, Mantissa, VA), and cells were cultured in in Dulbecco's modified Eagle's medium (DMEM)/F12 medium (Hyclone, Grand Island, NY, US) supplemented with 10% fetal bovine serum (FBS; Gibco, Grand Island, NY, US) at 37°C under 5% CO_2. The cells were used at passages 15-20, and all experiments were performed in serum-free medium.

Cell apoptosis and cell cycle assay

ARPE-19 cells (1×10^6) were seeded in 6-well plates and treated with BSA-AGE (50 μg/ml, 100 μg/ml, and 200 μg/ml) for 48 h. The cells were detached using ethylene diamine tetraacetic acid (EDTA), washed in ice-cold PBS (4°C), and treated with an FITC Annexin V Apoptosis Detection Kit or BD Cycletest™Plus DNA Reagent Kit according to the manufacturer's protocol. Samples were analyzed using a FACSCalibur cytometer (Becton Dickinson, US). All experiments were performed in triplicate.

Morphology observation and immunofluorescencestaining

After ARPE-19 cells were treated with BSA-AGE (50 μg/ml, 100 μg/ml, and 200 μg/ml) for 48 h, cell morphology was observed and photographed with an inverted phase-contrast microscope (Olympus, Tokyo, Japan). For immunocytochemistry, cells were washed and fixed in 4% (v/v) paraformaldehyde for 15 min at room temperature. Then, the cells were blocked in 10% goat serum with 0.1% Triton X-100, followed by incubation with primary antibodies against fibronectin diluted to 1:100 at 4°C overnight. After being washed three times with PBS, the cells were incubated with FITC-conjugated secondary antibodies (1:500) at room temperature for 1 h. Nuclei were counterstained with 4', 6'-diamidino-2-phenylindole hydrochloride (DAPI) for 5 min. Images were acquired witha fluorescence microscope (Leica).

Cell proliferation assay

Cells were seeded onto 96-well microplates (2×10^3 cells per well). The CCK-8 assay was used to measure cell viability at 0 h, 12 h, 24 h, 48 h, and 72 h according to the manufacturer's instructions. Ten microliters of CCK-8 solution was added to each well, and cells were further incubated for 2.5 h. The optical density was measured at 450 nm with a microplate reader (Finstruments Multiskan Models 347; MTX Lab Systems, Inc., Vienna, VA). All experiments were performed in triplicate.

Quantitative real-time PCR analysis

Total RNA was isolated with TRIzol (Invitrogen, Carlsbad, CA, US) according to the manufacturer's protocol. Real-time quantitative PCR analysis was performed using IQ Supermix (Bio-

Rad, Hercules, CA). The following primers were used: p-ERK forward, 5'-CTG AAA TGC GCA CAG TTG CT-3', and reverse, 5'-CCT GTC AGT TCA GCC AAC CT-3'; ZO-1 forward, 5'-GTG TTG TGG ATA CCT TGT-3', and reverse, 5'-GAT GAT GCC TCG TTC TAC-3'; fibronectin forward, 5'-AGC GGA CCT ACC TAG GCA AT-3', and reverse, 5'-GGT TTG CGA TGG TAC AGC TT-3'; glyceraldehyde phosphate dehydrogenase (GAPDH) forward, 5'-GAA GGT GAA GGT CGG AGT C-3', and reverse, 5'-GAA GAT GGT GAT GGG ATT TC-3' (Sangon. Shanghai, China). The amplification and thermo-cycling procedures were conducted according to the manufacturer's instructions. GAPDH served as the reference gene for quantity control. Experiments were performed in triplicate and repeated at least three times.

Western blot analysis

Cell proteins were prepared with a total protein extraction kit (Amsbio, Abingdon, UK), followed by protein concentration measurements with a BCA Protein Assay Kit (Pierce, Rockford, IL, US). Equal amounts of protein were separated by 10% sodium dodecyl sulfate polyacrylamide gels, transferred to polyvinylidene difluoride filters, and visualized with enhanced chemiluminescence detection reagents (Pierce). Bands were quantified using Quantity One software (Bio-Rad, Richmond, CA, US) and normalized to that of β-actin. All immunoblot analyses were repeated three times, and similar results were obtained.

Cytometric bead array

The concentrations of interleukin 1β, 6, 8, 10, and 12p (IL-1β, IL-6, IL-8, IL-10, and IL-12p) and tumor necrosis factor-alpha (TNF-α) in ARPE-19 cell supernatants were measured with a cytometric bead array (CBA, No. 552932; BD Bioscience, San Jose, CA, US) as previously described [16]. Briefly, cell supernatants were collected and centrifuged at 12,000×g at 4°C. Then 50 μl of the supernatant sample was used for each test and measured with flow cytometry (BD FACSCalibur, BD Bioscience). The concentration of each cytokine was calculated according to the protocol of the CBA kit.

Cell migration assay

The ARPE-19 cell migration assay was performed using a Transwell chamber. Briefly, 2×10^4 cells in 200 μl serum-free medium were placed in the upper chamber, whereas 600 μl DMEM with 10% FBS was in the bottom chamber. All migration assays were conducted for 6 h at 37°C. Then, cells were fixed in 4% paraformaldehyde and stained with DAPI for 15 min. After removal of the non-migrating cells with a cotton swab, the membrane was imaged and cells from five random fields of view were counted. Each experiment was repeated three times.

Statistical analysis

Data were expressed as the mean ± standard deviation (SD). Statistical analysis was conducted using Prism 5 (GraphPad Software, Inc., San Diego, CA, US). Differences were evaluated using a one-way analysis of variance (ANOVA) followed by Tukey's multiple comparison test or using an unpaired Student t-test. $P<0.05$ was considered statistically significant.

Results

Effects of AGEs on cell apoptosis and the cell cycle

We first evaluated the effects of AGEs on ARPE-19 cell apoptosis (early and late apoptosis) and cell cycle arrest (G2/M, S and G1 phase). AGEs induced cell apoptosis and cell cycle arrest in a dose-dependent manner. As shown in **Figure 1A**, cells treated with 100 μg/ml and 200 μg/ml AGEs displayed a significant increase in cell apoptosis compared to controls, whereas there was no significant difference among 50 μg/ml AGEs, BSA and control groups. Additionally, AGEs at a dose of 200 μg/ml resulted in a significant accumulation of ARPE-19 cells in the G1 phase and a reduction of cells in the G2/M and S phase compared to controls ($P<0.01$; **Figure 1B**). However, there was no significant difference among 100 μg/ml AGEs, 50 μg/ml AGEs, BSA and control groups in the cell cycle test ($P>0.05$; **Figure 1B**).

Effects of AGEs on cell morphology and fibronectin expression

Transforming growth factor-beta (TGF-β) is regarded as a major and potent inducer of EMT [17]. To investigate whether AGEs were associated with ARPE-19 cell phenotype changes, TGF-β treatment was used as a positive control. In normal culture conditions, ARPE-19 cells had

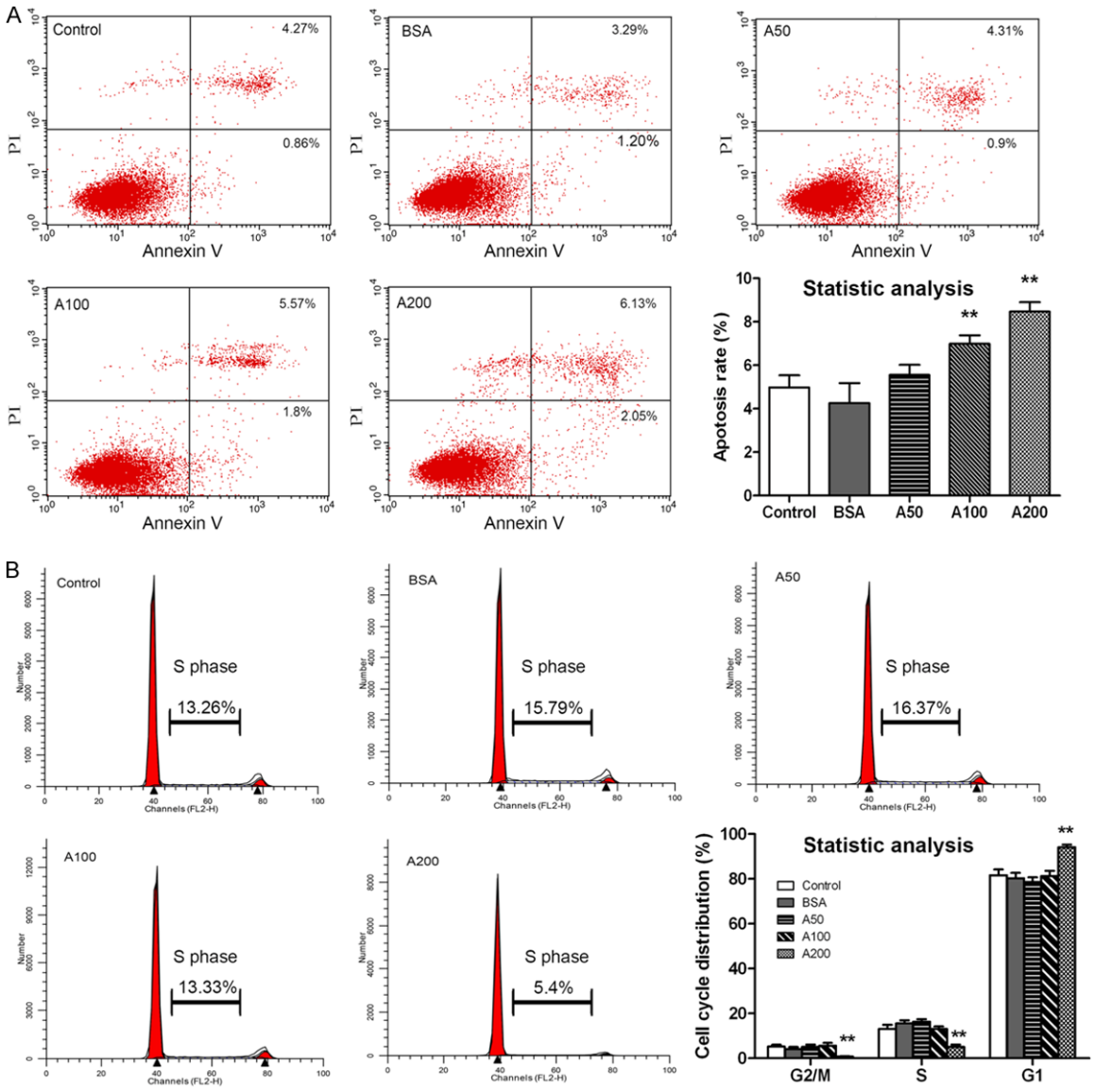

Figure 1. Effects of AGEs on RPE cell apoptosis and the cell cycle. A. Apoptosis of RPE cells treated with BAS or different concentrations of AGEs. Samples were taken 48 h after treatment, and cells were stained with Annexin V and PI for flow cytometry analysis. B. AGEs (200 μg/ml) induced cell cycle arrest in ARPE-19 cells. Samples were taken 48 h after BSA or AGEs treatment, and DNA content was analyzed with PI staining. The percentage of cells in the G2/M, S and G1 are indicated. Data are the mean ± SD of results from three independent experiments. $^{**}P<0.01$ vs. control.

a typical cobblestone-like epithelial morphology. As the concentrations of AGEs increased, cells gradually changed to a spindle fibroblast-like morphology (**Figure 2A**). In addition, fibronectin protein expression was enhanced with the increased AGEs concentration (**Figure 2B**). In contrast, BSA-treated cells retained their epithelial morphology and displayed slightly strengthened fibronectin expression (**Figure 2**).

AGEs induced the EMT in ARPE-19 cells via ERK phosphorylation

Because we had observed an association among AGEs, phenotypic transition and fibronectin expression in ARPE-19 cells, we next sought to examine whether AGEs could induce the EMT. Cells were treated with various doses of AGEs for 12 h, 24 h, 48 h and 72 h. As shown in **Figure 3A**, cell proliferation was significantly

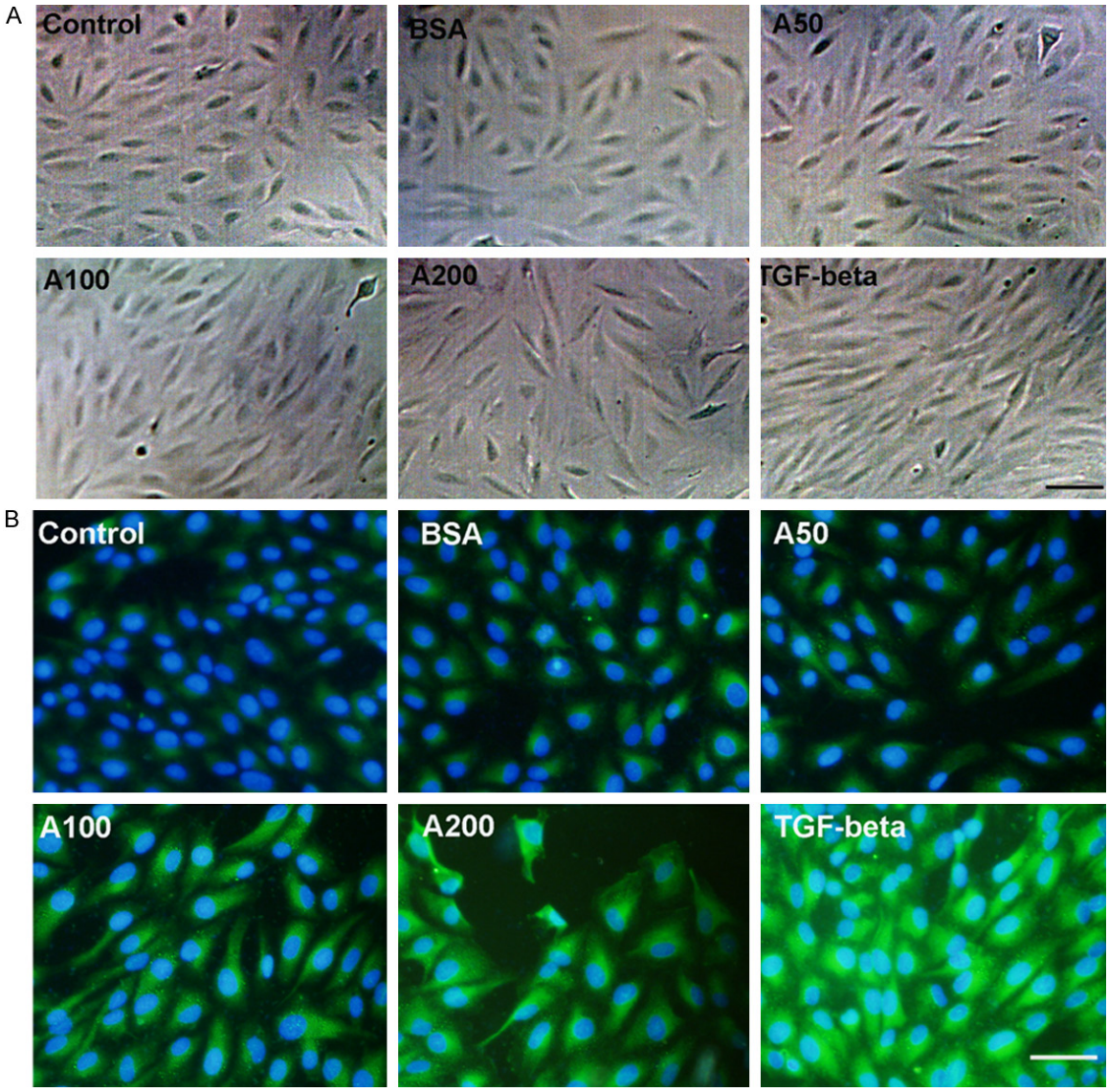

Figure 2. Morphologic changes of ARPE-19 cells and immunofluorescence staining for fibronectin by AGEs treatment. A. ARPE-19 cell morphology was assessed after exposure to BSA or AGEs for 48 h. Control and BSA-treated cells retained the oval cell morphology, whereas AGEs-treated cells gradually turned to a spindle mesenchymal phenotype in a dose-dependent manner. B. Fibronectin expression was assessed by immunofluorescence. The secondary antibody for fibronectin was labeled by FITC (green), and cell nuclei were stained with DAPI (blue). Fibronectin was positively expressed in the cytoplasm of ARPE-19 cells and up-regulated dose dependently by AGEs treatment. TGF-β was used for the positive control. DAPI: 4', 6'-diamino-2-phenylindole. Scale bars, 50 mm.

decreased with AGEs treatment of all doses at 48 h (P<0.01) and with 200 μg/ml of AGEs treatment at 72 h (P<0.05) compared to controls. However, there was no significant difference in cell proliferation between cells exposed to BSA and controls at all checked time-points (P>0.05).

Then, we explored the expression of certain epithelial and mesenchymal markers in ARPE-19 cells treated with 100 μg/ml AGEs for 48 h. RT-PCR demonstrated that AGEs treatment significantly induced a decrease in ZO-1 expression and an increase in fibronectin and p-ERK expression at an mRNA level compared to the BSA group (**Figure 3B**, P<0.01). The Western blot results further confirmed these changes (**Figure 3C** and **3D**). Therefore, we employed the MEK/ERK inhibitor U0126 to investigate the role of ERK activation in AGEs-induced EMT. U0126 successfully inhibited the ERK phos-

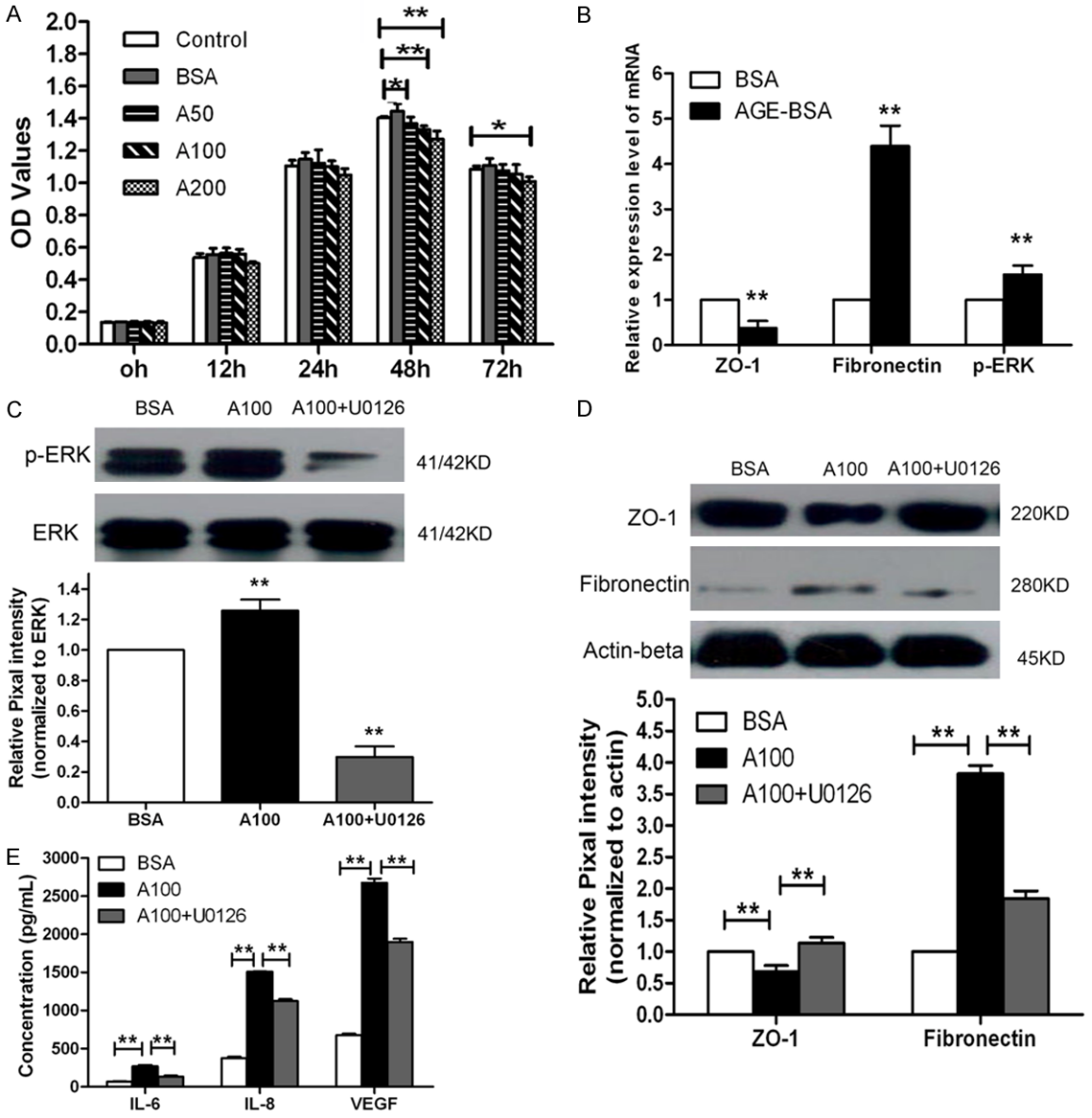

Figure 3. Effects of AGEs on the EMT in ARPE-19 cells. (A) Cells were treated with various concentrations of AGEs (50 μg/ml, 100 μg/ml, and 200 μg/ml) for 12 h, 24 h, 48 h and 72 h, and cell proliferation was analyzed using a CCK-8 assay. (B) Cells were treated with 100 μg/ml AGEs or BSA for 48 h, and the expressions of ZO-1, fibronectin and p-ERK were detected by RT-PCR. GAPDH was used as a loading control. (C) Cells were treated with 100 μg/ml BSA or 100 μg/ml AGEs in the presence or absence of a pretreatment of 30 min with U0126 (10 μM) for 48 h. Representative Western blot showing that AGEs enhanced ERK phosphorylation, which was compromised significantly by U0126. (D) Cells were treated as described in (C), and the protein levels of ZO-1 and fibronectin were determined by Western blot assay. β-actin was used as a loading control. (E) Cells were treated as described in (C), and the concentrations of EMT-related cytokines (IL-6, IL-8 and VEGF) in the culture supernatants were quantified with a CBA assay. AGEs increased the expression of those cytokines, which was partly blocked by U0126. Data are shown as the mean ± SD, n=3 experiments. $^{*}P<0.05$,$^{**}P<0.01$. BSA was set to 100% in (B-D).

phorylation (**Figure 3C**, $P<0.01$) and attenuated AGEs-caused protein expression changes of ZO-1 and fibronectin (**Figure 3D**, $P<0.01$).

Furthermore, the CBA method was used to determine the concentrations of secreted IL-1β, IL-6, IL-8, IL-10, IL-12p, VEGF and TNF-α. Our results showed that the production of IL-6, IL-8 and VEGF was significantly higher in the AGEs treatment group compared to the BSA group, and those enhanced productions were significantly weakened by U0126 (**Figure 3E**, $P<0.01$).

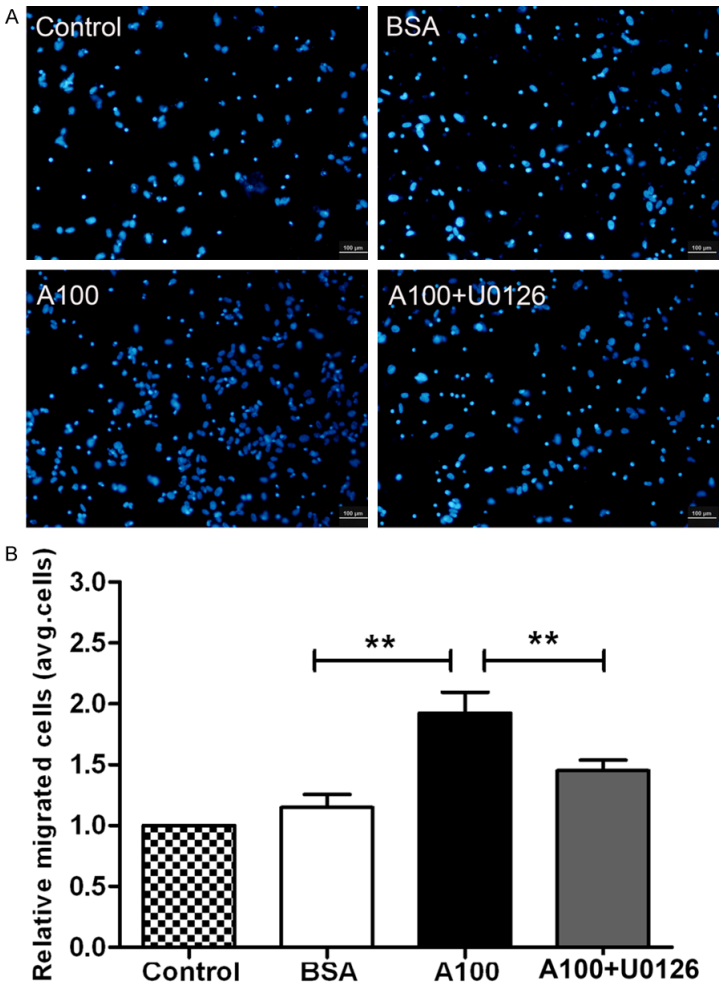

Figure 4. Effects of AGEs on ARPE-19 cell migration. Cells were left untreated or treated with 100 μg/ml BSA, or 100 μg/ml AGEs in the presence or absence of a pre-treatment of 30 min with U0126 (10 μM) for 48 h, and then cell migratory activity was determined with a Transwell assay. A. Representative images of cells migrated through the filter of the chamber. B. Statistical analysis based on the number of migrated cells. AGEs promoted cell migration significantly, whereas U0126 impaired the migration activity in the presence of AGEs (100 μg/ml). Data are shown as the mean ± SD, n=4 experiments. $^{**}P<0.01$. Controls were set at 100%.

However, there was no significant difference in the secretion of other cytokines examined among those three groups, such as IL-1β and TNF-α (data not shown). Collectively, these results suggested that ARPE-19 cells had undergone EMT in response to AGEs treatment via ERK activation.

AGEs promoted ARPE-19 cell migration

Because enhanced migration is an important characteristic of the EMT, we next examined the migration of ARPE-19 cells. As shown in **Figure 4**, cellular migration activity was increased by approximately 2-fold in the AGEs group compared with that of the control and BSA groups ($P<0.01$). As expected, the migration capability of ARPE-19 cells in the AGEs group was significantly compromised by U0126 treatment ($P<0.01$). However, no significant difference was observed between the control and BSA groups.

Discussion

In the present study, we have for the first time, to our knowledge, provided direct evidence that AGEs induced an EMT in ARPE-19 cells, which was characterized by a phenotype transition to a mesenchymal-like appearance, decreased ZO-1 expression, increased fibronectin expression, strengthened EMT-related cytokine production and enhanced cell migration capability. Our data also showed the effect of AGEs on EMT through ERK activation, as U0126 partly blocked those EMT changes. Furthermore, we demonstrated that higher concentrations of AGEs could result in apoptosis and cell cycle arrest in ARPE-19 cells.

AGEs have been previously reported to induce cell apoptosis [18]. Here, we first verified the effects of different concentrations of AGEs in the RPE cells and determined the appropriate dose of AGEs for further experiments. Our results showed that doses of AGEs higher than 100 μg/ml led to significant cell apoptosis and cell cycle arrest at the G1 phase (**Figure 1**). Next, we explored the appropriate doses of AGEs for ARPE-19 cell phenotypic changes and fibronectin expression. As the concentrations of AGEs increased, RPE cells gradually changed from the cobblestone-like shape to a spindle fibroblast-like morphology and gradually displayed intensive expression of fibronectin (**Figure 2**). Based on our results, we chose 100 μg/ml AGEs for further studies, which was similarto

the doses used in many other*in vitro* studies [18, 19].

Because AGEs induced EMT phenotype changes in ARPE-19 cells, we next examined the effect of AGEs on the expression of EMT markers and cellular migration activity. Tamiya et al. [20] strongly suggested that a loss of cell-cell adhesion was responsible for initiating the EMT and the proliferation of RPE cells. ZO-1 is key to the maintenance of an epithelial phenotype, and a loss of ZO-1 is considered a hallmark of the EMT. We also demonstrated the down-regulation of ZO-1 by AGEs (100 μg/ml) treatment for 48 h. The loss of ZO-1 has also been reported in EMTs occurring in other organic diseases, such as pulmonary fibrosis [21]. When epithelial cells initiate the EMT, they lose epithelial proteins while elevating the synthesis of cytoskeletal proteins [22]. The expression of fibronectin, a mesenchymal marker, was also up-regulated by AGEs treatment in ARPE-19 cells. Similarly, the effect of AGEs on EMT has been reported in diabetic nephropathy [19].

RPE cells secrete inflammatory or fibrosis-related cytokines, such as TNF-α, IL-6, VEGF and TGF-β, which trigger EMT changes [23]. The vitreous fluid of PDR patients contains a higher concentration of cytokines, including TGF-β, pentosidine (a sensitive marker for all AGEs) and IL-6, compared to that of non-diabetic patients [24, 25]. TGF-β is a potent chemoattractant in transforming RPE cells into mesenchymal fibroblastic cells [26]; thus, it was rational to use TGF-β as a positive control in our study and Zhu and co-workers' study [27]. IL-6 is a multifunctional cytokine, and Nakumura et al. [25] demonstrated that IL-6 levels in the vitreous of PDR patients were correlated with the severity of the disease. Cohen et al. [28] reported that IL-6 may increase the expression of VEGF. In addition, it has been reported that AGEs were involved in the development of diabetic retinopathy by enhancing the production of IL-6 and VEGF both *in vivo* and *in vitro* [14, 25, 29]. Similarly, our study found that AGEs increased the production of IL-6, IL-8 and VEGF in ARPE-19 cells.

The molecular mechanisms that govern EMT are complicated, with cross talk among signaling pathways such as the Smad pathway, Wnt pathway and Notch pathway [30]. Because AGEs are reported to be involved in the ERK pathways [31], we also used U0126, the inhibitor of ERK activation, to investigate whether AGEs induced EMT through the ERK pathway. Our data showed that U0126 partly blocked the EMT induced by AGEs in ARPE-19 cells by up-regulating the protein levels of ZO-1, down-regulating the protein expression of fibronectin, preventing the release of EMT-related factors, and impairing the cellular migration ability.

The limitations of this study should be noted. One limitation is that only in vitro experiments were carried out, as the animal model for PDR is not well established. Another limitation is that we focused on the ERK pathway in the present study, although other pathways, such as the Wnt pathway, should also be studied. Further studies are needed to elucidate all the possible pathways involved and their cross talk.

In conclusion, we have demonstrated that AGEs induced the EMT in ARPE-19 cells, at least in part through ERK activation. Moreover, we found that AGEs regulate cell apoptosis and the cell cycle in ARPE-19 cells while simultaneously inducing the EMT. Therefore, AGEs may be targeted for the treatment of human PDR.

Acknowledgements

This work was supported by the National Basic Research Program of China (973 Program, 2011CB510200) and the National Natural Science Foundation of China (Grant 81570858). The funders had no role in the study design, data collection and analysis, decision to publish or preparation of the manuscript.

Disclosure of conflict of interest

None.

Address correspondence to: Dr. Xiao-Xin Li, Department of Ophthalmology, Peking University People's Hospital, 11 South Avenue, Xizhimen, Xicheng District, Beijing 10044, China. Tel: +86 10 8832-5413; Fax: +86 10 68312393; E-mail: drlixiaoxin@163.com

References

[1] Nentwich MM, Ulbig MW. Diabetic retinopathy - ocular complications of diabetes mellitus. World J Diabetes 2015; 6: 489-499.

[2] Walshe R, Esser P, Wiedemann P, Heimann K. Proliferative retinal diseases: myofibroblasts cause chronic vitreoretinal traction. Br J Ophthalmol 1992; 76: 550-552.
[3] Hiscott P, Hagan S, Heathcote L, Sheridan CM, Groenewald CP, Grierson I, Wong D, Paraoan L. Pathobiology of epiretinal and subretinal membranes: possible roles for the matricellular proteins thrombospondin 1 and osteonectin (SPARC). Eye (Lond) 2002; 16: 393-403.
[4] Hiscott PS, Grierson I, McLeod D. Retinal pigment epithelial cells in epiretinal membranes: an immunohistochemical study. Br J Ophthalmol 1984; 68: 708-715.
[5] Kalluri R, Weinberg RA. The basics of epithelial-mesenchymal transition. J Clin Invest 2009; 119: 1420-1428.
[6] Lee H, O'Meara SJ, O'Brien C, Kane R. The role of gremlin, a BMP antagonist, and epithelial-to-mesenchymal transition in proliferative vitreoretinopathy. Invest Ophthalmol Vis Sci 2007; 48: 4291-4299.
[7] Wynn TA, Ramalingam TR. Mechanisms of fibrosis: therapeutic translation for fibrotic disease. Nat Med 2012; 18: 1028-1040.
[8] Morescalchi F, Duse S, Gambicorti E, Romano MR, Costagliola C, Semeraro F. Proliferative vitreoretinopathy after eye injuries: an overexpression of growth factors and cytokines leading to a retinal keloid. Mediators Inflamm 2013; 2013: 269787.
[9] Chen X, Xiao W, Liu X, Zeng M, Luo L, Wu M, Ye S, Liu Y. Blockade of Jagged/Notch pathway abrogates transforming growth factor beta2-induced epithelial-mesenchymal transition in human retinal pigment epithelium cells. Curr Mol Med 2014; 14: 523-534.
[10] Wei Q, Ren X, Jiang Y, Jin H, Liu N, Li J. Advanced glycation end products accelerate rat vascular calcification through RAGE/oxidative stress. BMC Cardiovasc Disord 2013; 13: 13.
[11] Pachydaki SI, Tari SR, Lee SE, Ma W, Tseng JJ, Sosunov AA, Cataldergirmen G, Scarmeas N, Caspersen C, Chang S, Schiff WM, Schmidt AM, Barile GR. Upregulation of RAGE and its ligands in proliferative retinal disease. Exp Eye Res 2006; 82: 807-815.
[12] Wang J, Xu X, Elliott MH, Zhu M, Le YZ. Muller cell-derived VEGF is essential for diabetes-induced retinal inflammation and vascular leakage. Diabetes 2010; 59: 2297-2305.
[13] Ma W, Lee SE, Guo J, Qu W, Hudson BI, Schmidt AM, Barile GR. RAGE ligand upregulation of VEGF secretion in ARPE-19 cells. Invest Ophthalmol Vis Sci 2007; 48: 1355-1361.
[14] Treins C, Giorgetti-Peraldi S, Murdaca J, Van Obberghen E. Regulation of vascular endothelial growth factor expression by advanced glycation end products. J Biol Chem 2001; 276: 43836-43841.
[15] Chen XL, Zhang XD, Li YY, Chen XM, Tang DR, Ran RJ. Involvement of HMGB1 mediated signalling pathway in diabetic retinopathy: evidence from type 2 diabetic rats and ARPE-19 cells under diabetic condition. Br J Ophthalmol 2013; 97: 1598-1603.
[16] Yoshida S, Kubo Y, Kobayashi Y, Zhou Y, Nakama T, Yamaguchi M, Tachibana T, Ishikawa K, Arita R, Nakao S, Sassa Y, Oshima Y, Kono T, Ishibashi T. Increased vitreous concentrations of MCP-1 and IL-6 after vitrectomy in patients with proliferative diabetic retinopathy: possible association with postoperative macular oedema. Br J Ophthalmol 2015; 99: 960-966.
[17] Border WA, Noble NA. Transforming growth factor beta in tissue fibrosis. N Engl J Med 1994; 331: 1286-1292.
[18] Wang XL, Yu T, Yan QC, Wang W, Meng N, Li XJ, Luo YH. AGEs Promote Oxidative Stress and Induce Apoptosis in Retinal Pigmented Epithelium Cells RAGE-dependently. J Mol Neurosci 2015; 56: 449-460.
[19] Bai YH, Wang JP, Yang M, Zeng Y, Jiang HY. SiRNA-HMGA2 weakened AGEs-induced epithelial-to-mesenchymal transition in tubular epithelial cells. Biochem Biophys Res Commun 2015; 457: 730-735.
[20] Tamiya S, Liu L, Kaplan HJ. Epithelial-mesenchymal transition and proliferation of retinal pigment epithelial cells initiated upon loss of cell-cell contact. Invest Ophthalmol Vis Sci 2010; 51: 2755-2763.
[21] Willis BC, Liebler JM, Luby-Phelps K, Nicholson AG, Crandall ED, du Bois RM, Borok Z. Induction of epithelial-mesenchymal transition in alveolar epithelial cells by transforming growth factor-beta1: potential role in idiopathic pulmonary fibrosis. Am J Pathol 2005; 166: 1321-1332.
[22] Zeisberg M, Neilson EG. Biomarkers for epithelial-mesenchymal transitions. J Clin Invest 2009; 119: 1429-1437.
[23] Holtkamp GM, Kijlstra A, Peek R, de Vos AF. Retinal pigment epithelium-immune system interactions: cytokine production and cytokine-induced changes. Prog Retin Eye Res 2001; 20: 29-48.
[24] Abcouwer SF. Angiogenic Factors and Cytokines in Diabetic Retinopathy. J Clin Cell Immunol 2013; Suppl 1.
[25] Nakamura N, Hasegawa G, Obayashi H, Yamazaki M, Ogata M, Nakano K, Yoshikawa T, Watanabe A, Kinoshita S, Fujinami A, Ohta M, Imamura Y, Ikeda T. Increased concentration of pentosidine, an advanced glycation end product, and interleukin-6 in the vitreous of patients with proliferative diabetic retinopathy. Diabetes Res Clin Pract 2003; 61: 93-101.

[26] Chung EJ, Chun JN, Jung SA, Cho JW, Lee JH. TGF-beta-stimulated aberrant expression of class III beta-tubulin via the ERK signaling pathway in cultured retinal pigment epithelial cells. Biochem Biophys Res Commun 2011; 415: 367-372.

[27] Zhu L, Li X, Chen Y, Fang J, Ge Z. High-mobility group box 1: a novel inducer of the epithelial-mesenchymal transition in colorectal carcinoma. Cancer Lett 2015; 357: 527-534.

[28] Cohen T, Nahari D, Cerem LW, Neufeld G, Levi BZ. Interleukin 6 induces the expression of vascular endothelial growth factor. J Biol Chem 1996; 271: 736-741.

[29] Hirata C, Nakano K, Nakamura N, Kitagawa Y, Shigeta H, Hasegawa G, Ogata M, Ikeda T, Sawa H, Nakamura K, Ienaga K, Obayashi H, Kondo M. Advanced glycation end products induce expression of vascular endothelial growth factor by retinal Muller cells. Biochem Biophys Res Commun 1997; 236: 712-715.

[30] Lovicu FJ, Shin EH, McAvoy JW. Fibrosis in the lens. Sprouty regulation of TGFbeta-signaling prevents lens EMT leading to cataract. Exp Eye Res 2016; 142: 92-101.

[31] Li JH, Wang W, Huang XR, Oldfield M, Schmidt AM, Cooper ME, Lan HY. Advanced glycation end products induce tubular epithelial-myofibroblast transition through the RAGE-ERK1/2 MAP kinase signaling pathway. Am J Pathol 2004; 164: 1389-1397.